Plant Physiology and Biochemistry 168 (2021) 116–127

Contents lists available at ScienceDirect

Plant Physiology and Biochemistry

journal homepage: www.elsevier.com/locate/plaphy

Physiological, metabolic, and stomatal adjustments in response to salt stress in *Jatropha curcas*

Marcelo F. Pompelli [a,*], Pedro P.B. Ferreira [b], Agnaldo R.M. Chaves [c], Regina C.Q. Q. Figueiredo [d], Auxiliadora O. Martins [e], Alfredo Jarma-Orozco [a], Arvind Bhatt [f], Willian Batista-Silva [e], Laurício Endres [g], Wagner L. Araújo [e,**]

[a] *Grupo Regional de Investigación Participativa de los Pequeños Productores de la Costa Atlantica. Universidad de Córdoba, Carrera 6 No. 77- 305 Montería, Córdoba, Colombia*
[b] *Pós-Graduação em Botânica, Universidade Federal Rural de Pernambuco, Recife, PE, Brazil*
[c] *Embrapa Semiárido, Petrolina, PE, Brazil*
[d] *Centro de Pesquisas Aggeu Magalhães/FIOCRUZ, Departamento de Microbiologia, Recife, PE, Brazil*
[e] *Departamento de Biologia Vegetal, Universidade Federal de Viçosa, Viçosa, MG, Brazil*
[f] *Lushan Botanical Garden, Chinese Academy of Science, Jiujiang, China*
[g] *Laboratório de Fisiologia Vegetal, Centro de Agronomia, Universidade Federal de Alagoas, Maceió, AL, Brazil*

ARTICLE INFO

Keywords:
Abiotic stress
Gas exchange
Metabolite reprogramming
NaCl
Physic nut
Stomatal functioning

ABSTRACT

Salinity is a major issue affecting photosynthesis and crop production worldwide. High salinity induces both osmotic and ionic stress in plant tissues as a result of complex interactions among morphological, physiological, and biochemical processes. Salinity, in turn, can provoke inactivation of some enzymes in the Calvin-Benson cycle and therefore affect the fine adjustment of electron transport in photosystem I and carbon related reactions. Here, we used three contrasting *Jatropha curcas* genotypes namely CNPAE183 (considered tolerant to salinity), CNPAE218 (sensible), and JCAL171 (intermediate) to understand salinity responses. By performing a long-term (12 months) experiment in land conditions, we investigated distinct mechanisms used by *J. curcas* to cope with threatening salinity effects by analyzing gas exchange, mineral nutrition and metabolic responses. First, our results highlighted the plasticity of stomatal development and density in *J. curcas* under salt stress. It also demonstrated that the CNPAE183 presented higher salt-tolerance whereas CNPAE218 displayed a more sensitive salt-tolerance response. Our results also revealed that both tolerance and sensitivity to salinity were connected with an extensive metabolite reprogramming in the Calvin-Benson cycle and Tricarboxylic Acid cycle intermediates with significant changes in amino acids and organic acids. Collectively, these results indicate that the CNPAE183 and CNPAE218 genotypes demonstrated certain characteristics of salt-tolerant-like and salt-sensitive-like genotypes, respectively. Overall, our results highlight the significance of metabolites associated with salt responses and further provide a useful selection criterion in during screening for salt tolerance in *J. curcas* in breeding programmes.

1. Introduction

Jatropha curcas L. (Euphorbiaceae) is an important and widely recognized promising source for bioenergy production. Thus, the production of *Jatropha* oil has enormous potential to contribute to the growing needs for energy resources (Pandey et al., 2012; Lozano-Isla et al., 2018; Reubens et al., 2011). This species is native to Central America or Mexico and widely distributed in tropical and subtropical region of Central and South America, Africa, India and Southeast Asia (Schmook et al., 1997). *J. curcas* have ability to grow rapidly, adaptability to different agro-climatic conditions and able to produce fruits after 9–12 months after planting and therefore the cost of seeds is low (Corte-Real et al., 2016; Silitonga et al., 2017). Previous studies reported that a single unimproved genetic *Jatropha* plant can yield more than 2.5 kg of seeds with a high oil content (30–50%) (Pandey et al., 2012; Pompelli et al., 2010a). For example, 1,250 plants can be cultivated in 1

* Corresponding author.
** Corresponding author.
E-mail addresses: mfpompelli@gmail.com (M.F. Pompelli), wlaraujo@ufv.br (W.L. Araújo).

https://doi.org/10.1016/j.plaphy.2021.09.039
Received 7 June 2021; Received in revised form 17 September 2021; Accepted 29 September 2021
Available online 2 October 2021

ha (spaced 4 × 2 m apart), producing from 0.937 to 1.25 tons of oil per hectare, whereas, soybeans (*Glycine max*) produce an average of 0.5 ton of oil per hectare. Moreover, the potential lifespan of *J. curcas* is 30–50 years and therefore it can be exploited commercially for a long period (Laviola et al., 2018) and also have ability to survive on infertile and degraded soils, protecting it against erosion (Lozano-Isla et al., 2018; Reubens et al., 2011; Pompelli et al., 2010b).

Although *J. curcas* is relatively drought-tolerant (Pompelli et al., 2010b; Hsie et al., 2015; Silva et al., 2015), it is also considered salt-sensitive (Lozano-Isla et al., 2018; Campos et al., 2012; Cerqueira et al., 2019; Corte-Real et al., 2020). It has been estimated that soil and water salinity is pervasive throughout the globe, reaching ~830 to 950 million hectares (Rengasamy, 2010), or approximately 20% of the total irrigated land area in the world (Huang et al., 2019). *J. curcas* can be cultivated in both arable and semiarid areas (Reubens et al., 2011; Hsie et al., 2015; Alburquerque et al., 2017), although irrigation is necessary in the latter. However, irrigation can lead to salinity caused by the salts introduced by irrigation water (Rengasamy, 2010). In this way, irrigation malpractices, particularly in arid and semiarid climatic zones, should be carefully used to avoid an increase in soil salinization. Salinity and drought are the main abiotic factors that affect plant growth and productivity in arid region by imposing osmotic stress that can lead to the loss of cell turgor and disrupt its biological capacity (Cerqueira et al., 2019; Koca et al., 2007; Batista-Silva et al., 2018). Nevertheless, plants have evolved various physiological and biochemical strategies that enable them to cope with unfavorable environmental conditions (Tang et al., 2019). Accordingly, some plants have evolved sophisticated molecular mechanisms that's assist them to recognize and respond to these diverse signals by regulating various physiological process such as photosynthesis, ion efflux, synthesis of osmoregulatory substances, and reactive oxygen species (ROS) scavenging (Corte-Real et al., 2020; Huang et al., 2019; Cabral et al., 2020; Souza et al., 2020; Silva-Santos et al., 2019).

Lozano-Isla, Campos, Endres, Bezzera-Neto and Pompelli (Lozano-Isla et al., 2018) studied the salinity effects in five different *J. curcas* genotypes and showed that salinity is very harmful during seed germination, directly impacting both seed germination rate and mean germination time. These authors also observed that some genotypes are more tolerant than others, a fact that could be promising for future breeding programs. Previous studies additionally demonstrated that *J. curcas* have ineffective system of redistribution of Na^+ and Cl^- as well as exclusion mechanisms that can reduce the excessive salt accumulation in shoots under salinity (Silva et al., 2015; Cerqueira et al., 2019). Accordingly, the potential of *J. curcas* in terms of tolerance to salinity remains controversial. One of the reasons for this divergence can be related to the diversity of physiological responses among genotypes in different studies and a lack of high yielding variety (Niu et al., 2016). Therefore, knowledge of *J. curcas* mechanisms under salinity stress is clearly required for understanding and improving the stress tolerance (Cheng et al., 2014). Different genotypes of *J. curcas* are reported to have the various adaptive mechanisms that enable them to cope with salinity stress (Lozano-Isla et al., 2018; Corte-Real et al., 2019, 2020; Cabral et al., 2020; Souza et al., 2020; Silva-Santos et al., 2019). Here, we hypothesized that those genotypes present physiological characteristics of salt tolerance in such a way that can aid in the selection of elite genotypes. Therefore, our main goal was to elucidate physiological and metabolic responses to salt stress in *J. curcas* genotypes. To this end, we used three contrasting *Jatropha curcas* genotypes, namely, CNPAE183 (considered tolerant to salinity), CNPAE218 (sensible), and JCAL171 (intermediate), and investigated the distinct mechanisms used by those genotypes to cope with threatening salinity effects.

2. Material and methods

2.1. Plant material and environmental conditions

The experiment was performed in the Experimental Field of Bebedouro (9°09′S, 40°22′W and 365 m asl), Embrapa Semiárido, Petrolina, Pernambuco State, Brazil. The climate classification in that region is considered to have BSh in the Köppen classification (Koppen, 1948) with 280.33 mm of total annual rainfall scattered throughout the year (Proclima, 2020). During the entire experimental period, 158 mm of rainfall was registered (Supplementary Fig. S1). Mean monthly temperatures ranged from 18 °C in July to 39 °C in December. The relative humidity ranged from 26% in October to 88% in December (Supplementary Fig. S1). The soil of the study area was described as Red Argisol Eutrophic abrupt plinthic A moderate, medium texture hyperxerophilic relief plane (Aguiar Neto et al., 2014).

The global radiation intercepted by the plants varied widely during the experiment(Supplementary Fig. S2), reaching 1,011 Watts m^{-2} at 11:30 a.m. on August 06, 2017. However, when we consider the radiation intercepted by the plants accumulated over 24 h, November 2017 stands out with a cumulative radiation of 31.49 MJ m^{-2} day^{-1} whereas May 2017 was the month with lower radiation accumulated over 24 h, with 10.77 MJ m^{-2} day^{-1} (Supplementary Fig. S3).

Through previous results (Lozano-Isla et al., 2018; Corte-Real et al., 2019, 2020; Cabral et al., 2020; Souza et al., 2020), we selected three different genotypes of *Jatropha curcas*, namely, CNPAE183, considered tolerant to salinity, CNPAE218 considered sensible, and JCAL171 that presented an intermediate tolerance. Seeds of these genotypes provided by Embrapa Agroenergia, Brasília, DF were sterilized as described by Corte-Real, Oliveira, Jarma-Orozco, Fernandes, dos Santos, Endres, Calsa Jr and Pompelli (Corte-Real et al., 2020). Subsequently, the seeds were transferred into polypropylene trays as described by Lozano-Isla, Campos, Endres, Bezzera-Neto and Pompelli (Lozano-Isla et al., 2018). During the germination period, the seedlings received only water without the addition of NaCl. Then, seedlings were transplanted to the final site, namely 250-L barrels, filled with soil from the Petrolina region, as described above. The experimental setup was performed under a randomized block design containing three genotypes (CNPAE183, JCAL171, and CNPAE218), five salt concentrations in the irrigation water (0 dS m^{-1}, 2.5 dS m^{-1}, 5 dS m^{-1}, 7.5 dS m^{-1}, and 10 dS m^{-1}), and 5 replicates. In the base of each barrel, a tap was installed to drain excess water. We used an automated irrigation system containing, for each saline concentration, a 500-L water tank, a peristaltic pump and a channel system that carried the water by dripping to the plants. All plants were irrigated every other day using dripper tubes with a flow of 2.5-L h^{-1}, nominal diameter of 13 mm, with two drippers per plant, spaced 0.15 m apart (further details can be additionally seen in Supplementary Fig. S4). Irrigation was performed for 2 h per day by applying 10 L $plant^{-1}$ day^{-1}. In the first 45 days, the seedlings received fresh water, aiming to acclimate the seedlings to the new environment. Thereafter, the plants containing at least 10 pairs of expanded leaves were irrigated with the respective saline concentration. The plants were submitted to routine agricultural practices.

2.1.1. Scanning electron microscopy

Leaf fragments ~0.5 cm^2 of the 3rd attached fully expanded leaf from the apex were sampled in 6- and 12-month stressed plants and immediately fixed in Karnovsky solution (Karnovsky, 1965), prepared in 0.1 M cacodylate buffer (sodium cacodylate trihydrate, Sigma Aldrich, St. Louis, USA), pH 7.4 and 2.5% glutaraldehyde (part number G5882, Sigma Aldrich) for 60 h at 4 °C. The fragments were then treated with chloroform P.A. (part number C2432, Sigma Aldrich) for 45 min under ultrasonic sonication (Digital Ultrasonic Cleaner, GuangDong GT Ultrasonic Co., Ltd, Guangdong, China) for complete extraction of the epicuticular waxes and the cuticle, making epidermal cells more exposed. The treated leaf samples were observed by scanning electron

microscopy (SEM). Stomatal density (SD) was measured by using Salisbury equations (Salisbury, 1928) with modifications proposed by Pompelli, Martins, Celin, Ventrella and DaMatta (Pompelli et al., 2010c). However, stomatal area and stomatal pore aperture measurement were performed as described previously (Pompelli et al., 2010c).

2.1.2. Leaf gas exchange parameters and chlorophyll a fluorescence

Every 30 days, leaf gas exchange and chlorophyll *a* fluorescence were determined on the 3rd attached fully expanded leaf from the apex, using a portable open-flow infrared gas analyzer (LI-6400XT; LI-COR Inc., Lincoln, NE, USA) integrated fluorescence chamber heads (LI-6400-40; LI-COR Inc.). The net photosynthesis (A_N, μmol CO_2 m^{-2} s^{-1}), stomatal conductance (g_s, mmol H_2O m^{-2} s^{-1}), and internal CO_2 concentration (C_i, μmol CO_2 mol^{-1}) were obtained on 2-month-old *J. curcas* plants from November 2016 to November 2017 at approximately 09:00–11:00 h solar time, under a clear sky and under the leaf irradiance of saturation of 1,000 μmol m^{-2} s^{-1} (as previously tested by light curves versus A_N), fixed CO_2 concentration in 390 μmol mol^{-1} and air flow of 400 μmol s^{-1} (Corte-Real et al., 2019). The fluorescence analysis were carried out as described by Pompelli, Martins, Antunes, Chaves and DaMatta (Pompelli et al., 2010d).

2.1.3. Leaf mineral elements

Concentrations of chloride (Cl^-), sodium (Na^+) and potassium (K^+) were measured in the same leaf that used for measuring the net photosynthesis and for chlorophyll fluorescence analysis on 6- and 12-month stressed plants. Leaves were oven-dried at 60 °C for 72 h and then ground into a fine powder to pass a 40-mesh sieve, and nutrient contents were determined according Silva (2009).

2.1.4. Carbon isotope composition ($\delta^{13}C$)

In the same leaves used to leaf mineral analyses, the carbon isotope composition ($\delta^{13}C$) was calculated as:

$$\delta^{13}C\ (‰) = \left(\frac{R_{sample}}{R_{standard}} - 1\right) * 1000$$

where R_{sample} is the $^{13}C/^{12}C$ ratio in the sample and $R_{standard}$ is the $^{13}C/^{12}C$ ratio in the standard (PDB-Pee Belemnite) (Ehleringer et al., 1990).

2.1.5. Metabolic analysis and metabolite profile

Leaf samples of the 3rd leaflet were harvested of the 6- and 12-month stressed plants and flash-frozen in N_2 at −80 °C until analysis. The samples were lyophilized before metabolite extraction. Approximately 25 mg of dry leaves were subjected to methanolic extraction as described by Silva, Lichtenstein, Alseekh, Rosado-Souza, Conte, Suguiyama, Lira, Fanourakis, Usadel, Bhering, DaMatta, Sulpice, Araújo, Rossi, Setta, Fernie, Carrari and Nunes-Nesi (Silva et al., 2017). The chlorophyll contents were determined as previously described by Wellburn (1994). Total chlorophyll (a+b) as well as the chlorophyll ratio were calculated. Starch, sucrose, fructose, and glucose were measured according to the methodology described by Fernie, Roscher, Ratcliffe and Kruger (Fernie et al., 2001). In the Methanolic insoluble fraction were analyzed for their total amino acids (Yemm et al., 1955), malate (Nunes-Nesi et al., 2007), starch (Fernie et al., 2001) and total protein (Bradford, 1976). The content of all compounds were normalized for dry mass.

The levels of all other metabolites were quantified by gas chromatography-mass spectrometry (GC-MS) as previously described by (Lisec et al., 2006). The mass spectra were cross-referenced with those in the Golm Metabolome Database (Kopka et al., 2005).

2.2. Experimental design and statistical analyses

The experiments were conducted in a completely randomized block design with three genotypes (CNPAE183, JCAL171, and CNPAE218), five salt concentrations in the irrigation water (0 dS m^{-1}, 2.5 dS m^{-1}, 5 dS m^{-1}, 7.5 dS m^{-1}, and 10 dS m^{-1}), and 5 replicates. All the data were analyzed by repeated measures ANOVA and means were compared using a SNK test ($P < 0.05$) by Statistic version 14.0 (StatSoft, Tulsa, OK, USA).

3. Results

3.1. Photosynthetic parameters are affected in J. curcas under salinity

Under control conditions, no correlation was detected between SD and the inverse of the leaf area (Fig. 1A). However, under salt stress (10 dS m^{-1}), the leaves become smaller, with more compacted cells (Fig. 1B). Under these conditions, we observed an increased stomatal density coupled with decreased leaf area in the CNPAE183 genotype. By contrast, decreased stomatal density without large changes in the leaf area was found in both JCAL171 and CNPAE218 genotypes. Fig. 1C corroborates this assumption and further adds that the stomatal density of the CNPAE183 genotype increased by 2.1-fold linearly with saline concentration, whereas the stomatal density of the genotypes JCAL171 and CNPAE218 increase by 1.4-fold and 1.2-fold, respectively. More stomata on the leaf surface could represent a greater capacity for water loss. However, a strong reduction of 44% in stomatal opening (from 32.68 ± 0.45 $μm^2$ to 18.36 ± 0.16 $μm^2$) in the 10 dS m^{-1} CNPAE183 genotype was observed (Fig. 1D). On the other hand, the JCAL171 and CNPAE218 genotypes increased their stomatal opening, respectively, from 30.10 ± 0.50 $μm^2$ to 41.82 ± 0.47 $μm^2$ (39% increase) and 41.82 ± 0.47 $μm^2$ for 44.62 ± 0.70 $μm^2$ (6.7% increase). Stomata size was decreased by 23% in the CNPAE183 genotype, whereas in JCAL171 and CNPAE218 genotypes, the stomata size is increased by 22% and 7% (Fig. 1E). By comparing SD and stomatal size (Fig. 1F) we perceived that the largest SD *versus* lower stomatal size was observed in the CNPAE183, whereas, JCAL171 showed the lowest SD with higher stomatal size (Fig. 1F).

The net photosynthesis (A_N) and stomatal conductance (g_s) were strongly reduced with salinity regardless of genotype (Fig. 2; Suppl. Table S1). In 6-month salt-stressed plants, severe reductions (75%, 81%, and 68%) in A_N were observed in CNPAE183, JCAL171, and CNPAE218 genotypes, respectively (Fig. 2). As expected, these reductions are even higher in 12-month salt-stressed plants, where A_N decreased significantly 81%, 94%, and 143% (reaching negative values) in the same genotypes. In close agreement, g_s also decreased by approximately 42%, 69%, and 78% in 6-month salt-stressed plants and 77%, 30%, and 79% in 12-month salt-stressed plants of CNPAE183, JCAL171, and CNPAE218 genotypes, respectively.

To further understand the influence of *J. curcas* genotypes on salt stress tolerance, we calculated the intrinsic water use efficiency (WUE_i). Accordingly, decreases of 51.3%, 82.5%, and 7.7%, respectively in 6-months salt-stressed plants of CNPAE183, JCAL171, and CNPAE218 genotypes were observed (Fig. 3). Furthermore, in 12-month salt-stressed plants, the CNPAE183 genotype showed a moderate decrease in WUE_i (29%), while, in the JCAL171 and CNPAE218 genotypes the WUE_i fell abruptly to 92%, and 191%, respectively (reaching negative values; Fig. 3).

Decreases in WUE_i are modulated by g_s rather than A_N. In general, stomatal closure causes a decrease in $[CO_2]$ in the substomatal chamber and, consequently, a decrease in the C_i/C_a ratio. The C_i/C_a ratio was differently altered in both *J. curcas* genotypes (Fig. 3). As result, in 6-month salt-stressed plants, the C_i/C_a ratio increased by 33%, 10%, and 27% in the CNPAE183, JCAL171, and CNPAE218 genotypes, respectively (Fig. 3). Surprisingly, these ratios increased in 12-month salt-stressed plants by 67% (CNPAE183), 42% (CNPAE218), and 154% (JCAL171) (Fig. 3).

Although stomatal closure could provoke an increase in leaf temperature (T_{leaf}), this was not observed in *J. curcas*. When we compared 6-month salt-stressed plants with non-stressed plants of the same age, we

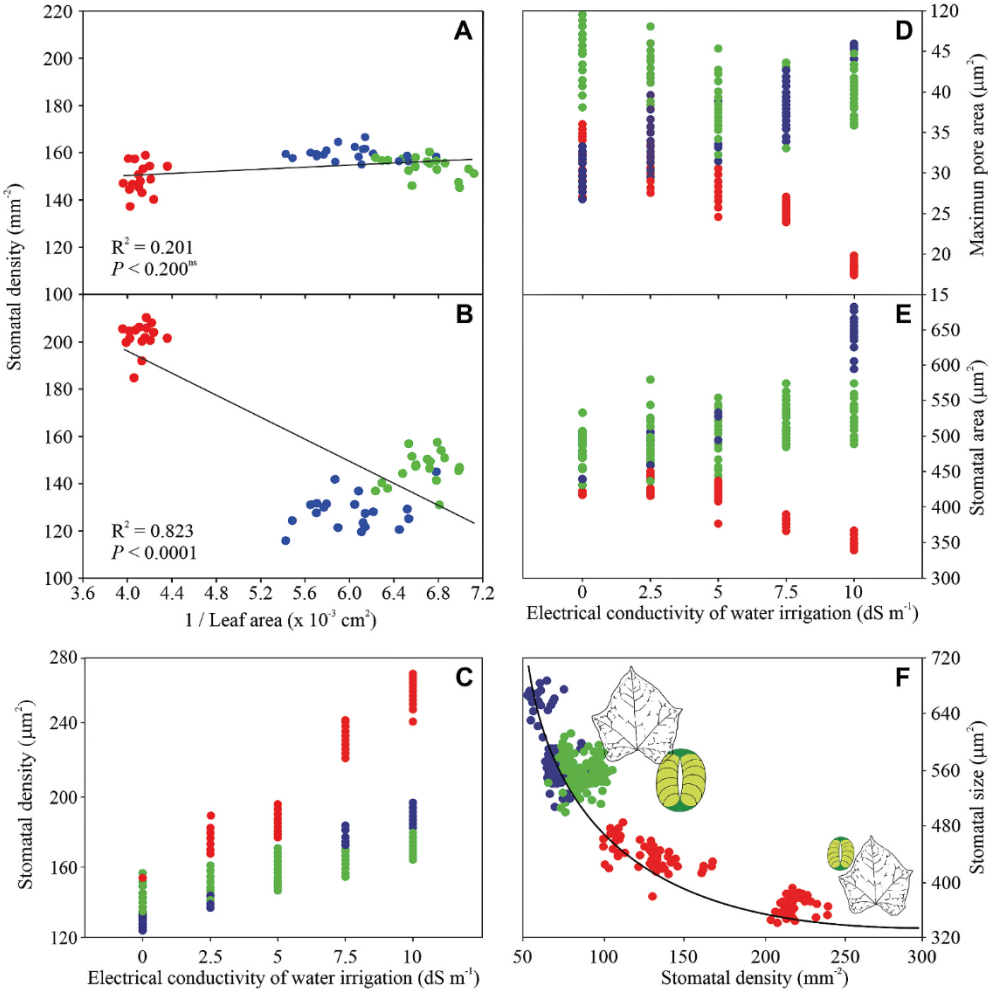

Fig. 1. Relationships between stomatal density and 1/leaf area (A–B) and between electrical conductivity in water irrigation and stomatal density (C), maximum pore area (D), stomatal area (E), and between stomatal size and stomatal density (F). Data was obtained in three genotypes (CNPAE183, red symbols; JCAL171, blue symbols; and CNPAE218, green symbols) of *Jatropha curcas* subjected to five concentration of NaCl (0 dS m^{-1}, 2.5 dS m^{-1}, 5 dS m^{-1}, 7.5 dS m^{-1} and 10 dS m^{-1}). Data represent the mean of 10 biological replicates per genotype. Equations: Stomatal density = 144.128 – (11.047 *[salt-CNPAE183]), R^2 = 0.970; Stomatal density = 130.570 + (5.506 *[salt-JCAL171]), R^2 = 0.966; Stomatal density = 143.547 + (2.487 * [salt-CNPAE218]), R^2 = 0.869; Maximum pore area = 33.938 – (1.355 * [salt-CNPAE183]), R^2 = 0.921; Maximum pore area = 30.223 + (1.133 * [salt-JCAL171]), R^2 = 0.864; Maximum pore area = 43.653 – (0.589 * [salt-CNPAE218]), R^2 = 0.542; Stomatal area = 460.594 - (10.664 * [salt-CNPAE183]), R^2 = 0.936; Stomatal area = 521.122 + (11.033 * [salt-JCAL171]), R^2 = 0.869; Stomatal area = 537.096 + (2.852 * [salt-CNPAE218]), R^2 = 0.465; Stomatal size = 136.81 + (50,570.83/stomatal density), R^2 = 0.868. (For interpretation of the references to color in this figure legend, the reader is referred to the Web version of this article.)

verified a decrease in T_{leaf} to 0.8%, 1.5%, and 0.9 in the CNPAE183, JCAL171, and CNPAE218 genotypes, respectively (Fig. 4). Moreover, in 12-month salt-stressed plants, T_{leaf} practically did not increase in CNPAE183 (3.2%) or CNPAE218 (9.8%) but a considerable increase was observed in JCAL171 (33.1%) (Fig. 4). We additionally observed an inverse effect of T_{leaf} and transpiration (T), with T_{leaf} increasing with increasing saline concentrations, whereas T decreased in the same proportion ($r = -0.505$; Supplementary data file). Namely, T decreased to 83%, 54%, and 57% in 6-month salt-stressed plants CNPAE183, JCAL171, and CNPAE218 genotypes, respectively, and to 41%, 66%, and 90% in 12-month salt-stressed plants (Fig. 4).

Fig. 5 shows that when salt increases, the carbon isotope discrimination ($\delta^{13}C$) is higher. In fact, in 6-month stressed plants, the CNPAE183, and JCAL171 genotypes discriminated 9.3% and 10.3%, respectively, less $^{13}CO_2$ than $^{12}CO_2$, whereas the genotype CNPAE218 discriminated 6.2% (not significant at $P \leq 0.05$; Fig. 5). In 12-month salt-stressed plants, $\delta^{13}C$ was reduced by 0.3%, 15.4%, and 10.6% in CNPAE183, JCAL171, and CNPAE218, respectively (Fig. 5).

To further elucidate the physiological performance of the genotypes to salinity, we compared the relationship between the electron transport rate (ETR) and A_N versus g_s. We observed that in 6-month stressed plants, A_N decreased by 75%, 81%, and 68% while ETR decreased by 35%, 44%, and 45%, respectively, in the CNPAE183, JCAL171, and CNPAE218 genotypes. With the steeper reduction in A_N than ETR, the ETR/A_N increases. We also observed that the CNPAE183 genotype had a higher ETR/A_N accompanied by lower g_s; meanwhile, CNPAE218 showed comparatively lower ETR/A_N ratios with higher g_s (Fig. 6A).

Vapor pressure deficit (VPD) had no significant effect on the maximum stomata pore area when all genotypes were compared together (Fig. 6B). This fact aside, it is clear that the genotype CNPAE183 (red symbols in Fig. 6B) showed a lower maximum pore area, even under high VPDs, while the genotype CNPAE218 (green symbols in Fig. 7B) showed a significantly larger maximum pore area under lower VPDs.

3.1.1. *Leaf mineral elements*

To further analyze the influence of salinity on mineral element absorption and availability, nutritional analysis were performed (Fig. 7). As expected, *J. curcas* plants treated with 10 dS m^{-1} showed a significant increase in both Na^+ and Cl^- leaf concentrations when compared with non-stressed plants. As the salt treatment exposure time increased from 6- to 12-months, there was a proportional increase in Na^+ and Cl^- cellular levels (Fig. 7). In 6-month salt-stressed leaves, the Na^+ concentrations increased 1.4-, 3.0-, and 3.9-fold, while Cl^- increased 1.4-, 1.4-, and 1.6-fold, respectively, for the CNPAE183, JCAL171, and CNPAE218 genotypes. In 12-month salt-stressed leaves, both ions increased 1.2-, 1.3-, and 3.1-fold to Na^+ and 1.6-, 1.5-, and 1.6-fold to Cl^-, respectively, in the CNPAE183, JCAL171, and CNPAE218 genotypes (Fig. 7).

3.1.2. *Metabolic analysis and metabolite profile*

In 6-month stressed plants, leaf chlorosis was evident especially in plants treated with high salt concentrations. Chlorosis and necrosis at leaf edges were widespread in 12-month stressed plants throughout the experiment (more info in graphical abstract). Our metabolite analysis successfully detected 19 amino acids, 4 organic acids, 9 sugars, and 4

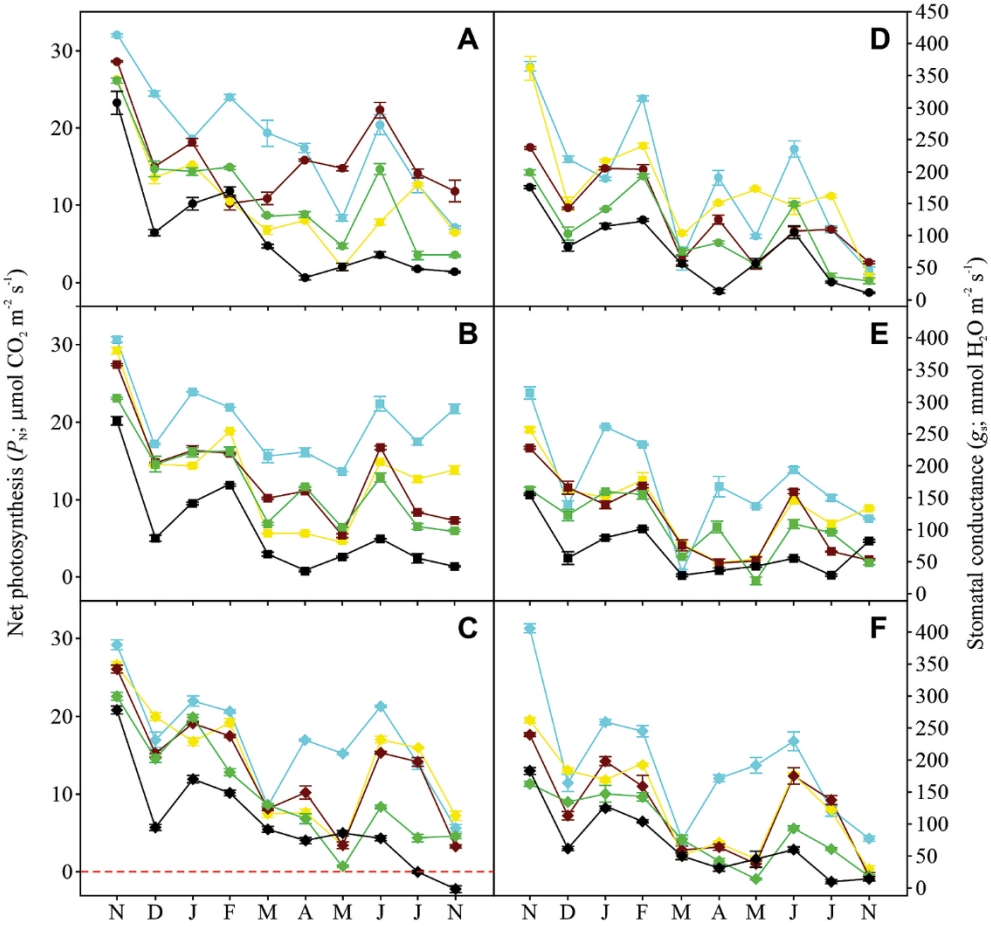

Fig. 2. Salt stress induced changes in gas exchange parameters in *Jatropha curcas*. Net photosynthesis (A–C) and stomatal conductance (D–F) measured in three genotypes (CNPAE183 – ●, A; JCAL171 – ■, B, and CNPAE218 – ◆ C) of *Jatropha curcas* during the experiment subjected to five concentration of salt [0 dS m^{-1} (cyan), 2.5 dS m^{-1} (yellow), 5 dS m^{-1} (brown), 7.5 dS m^{-1} (light green), and 10 dS m^{-1} (black)] in water irrigation. All data are expressed as means ± SE (n = 5). For statistical analysis, see Supplementary Table S1. Data below dotted line return negative values of net photosynthesis. (For interpretation of the references to color in this figure legend, the reader is referred to the Web version of this article.)

other compounds. The obtained data were displayed in false color in the heat map (Fig. 8) to provide an easy overview (the full data set is additionally available as Suppl. Table S2). Considerable changes in the levels of a wide range of organic acids, amino acids, and sugars were observed. The changes in metabolite profiles were, by and large, qualitatively similar between the genotypes, although quantitatively was rather variable (Fig. 8), as our data show that the salt-stress affected were more evident in 12-month plants than in 6-month stressed plants.

A Pearson correlation analysis was used for determining the relationship between different physiological parameters and tested salinity concentration. This was evident when we correlated salt versus chlorophyll (Chl) "a" (r = −0.352), Chl "b" (r = −0.273) and Chl total (r = −0.344). There was a strong negative correlation between salt concentration and protein level (r = −0.719), A_N (r = −0.512), Φ_{PSII} (r = −0.404), and ETR (r = −0.392). The strong positive correlation between salt concentration and Lysine (Lys) (r = 0.546) and negative correlation between Lys and Chl "a" (r = −0.612), Chl "b"(r = −0.866), Chl total (r = −0.470), or Sucrose (Suc; r = −0.609), Glucose 6-phosphate(G6P; r = −0.300), Isocitrate (Isoc; r = −0.418), Succinate (Succ; r = −0.379), and Malate (Mal; r = −0.820) were strong evidence of carbohydrate starvation, leading to catabolism of Lys. This idea is corroborated by a strong negative correlation between Lys and A_N (r = −0.456). Moreover, Lys was increased by 4.6-fold and 3.2-fold in CNPAE183 and JCAL171 and decreased by 74% in CNPAE218 in 12-month stressed plants. It is of interest that in general all free amino acids increased significantly in 12-month stressed plants of CNPAE183 and JCAL171, including Alanine (Ala), Asparagine (Asn), Aspartate (Asp), Cysteine (Cys), Lys, Glycine (Gly), Histidine (His), Serine (Ser), Threonine (Thr), Tyrosine (Tyr), Tryptophan (Trp), and Valine (Val), indicating an increased protein degradation under the experimental conditions (for more detail see Supplementary Data File).

Although we did not observed a significant correlation between Asn and salt stress, we noticed that 12-month stressed plants Asn accumulated 4.2-fold and 2.9-fold in CNPAE183 and JCAL171, respectively, but in the CNPAE218 genotype Asn was reduced by 58% at 10 dS m^{-1}. Glutamate (Glu) increased 1.4- and 2.5-fold in CNPAE183 and JCAL171 and decreased 17% in CNPAE218 genotype. The positive correlation between salt concentration and Glu($r = 0.445$) and negative correlation between Glu and Suc ($r = -0.208$), Glucose 6-phosphate (Glu6P; $r = -0.554$), Glyceraldehyde (Glyc; $r = -0.252$), Isoc ($r = -0.219$), Succ ($r = -0.364$), and Mal ($r = -0.243$) provide strong evidence of the catabolism of Glutamate.

The biosynthetic pathways of certain additional amino acids, namely, aromatic amino acids, as well as Ser, Arginine (Arg), Glutamine (Gln), and Ala, were also upregulated in CNPAE183 and JCAL171 and downregulated in CNPAE218 (Fig. 8). Serine biosynthesis is also upregulated in salt-stressed plants is in line with a high demand for Ser as a precursor of Trp synthesis. However, the strong positive correlation between salt concentration and Ser($r = 0.854$) or Gly ($r = 0.373$) is a strong indicator of increased photorespiration.This idea is corroborated by the strong negative correlation between Ser and Gly ($r = -0.605$). Another indication of the stress can be deduced by the elevation of two branched-chain amino acids, Lys and Thr, which were strongly increased in genotypes CNPAE183 and JCAL171 and decreased in CNPAE218 yet, in general, these amino acids had a strong correlation with the increase in salinity ($r = 0.545$ to Lys, and $r = 0.532$ to Thr).

Our results indicate that there might be a preference for fast degradation of specific amino acids in *J. curcas* plants subjected to salt stress to generate carbon skeletons to maintain mitochondrial respiration, and ATP production, due to carbohydrate starvation (more info in graphical

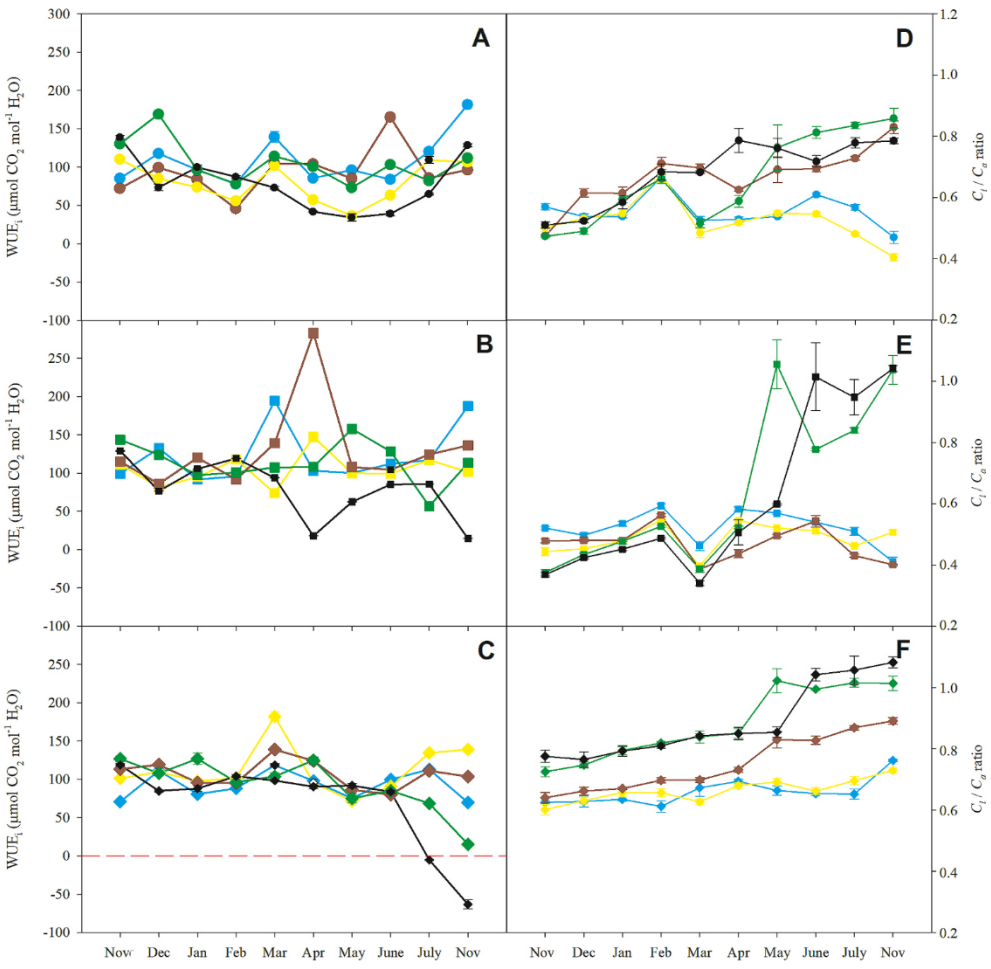

Fig. 3. Salt stress induced changes in WUE_i and C_i/C_a ratio in *Jatropha curcas*. Intrinsic water use efficiency ($WUE_i = A_N/g_s$; A-C) and internal-to-ambient CO_2 concentration (C_i/C_a ratio; D-F) measured in three genotypes (CNPAE183 – ●, A; JCAL171 – ■, B, and CNPAE218 – ◆ C) of *Jatropha curcas* subjected to five concentration of salt [0 dS m^{-1} (cyan), 2.5 dS m^{-1} (yellow), 5 dS m^{-1} (brown), 7.5 dS m^{-1} (light green), and 10 dS m^{-1} (black)] in water irrigation during the experiment. All data are expressed as means ± SE (n = 5). For statistical analysis, see Supplementary Table S1. Data below dotted line return negative values of intrinsic water use efficiency. (For interpretation of the references to color in this figure legend, the reader is referred to the Web version of this article.)

abstract) in response to low or negative A_N, as shown in Fig. 2. Further evidence of this mechanism is additionally obtained here. There is a strong positive correlation between salt concentration and Cys (r = 0.522) and a negative correlation between Cys and Suc (r = −0.290), G6P (r = −0.670), Glyc (r = −0.347), Isoc (r = −0.453), Succ (r = −0.625), Mal (r = −0.273), and Cit (r = −0.703) are strong evidence of the catabolism of Cys. A strong positive correlation between salt concentration and Arg (r = 0.751) and a negative correlation between Arg and G6P (r = −0.531), Glyc (r = −0.260), Isoc (r = −0.385), Succ (r = −0.398), and Mal (r = −0.493) indicate the metabolization of Arg. Finally, there was a mild positive correlation between salt concentration and Tyr (r = 0.396) and a negative correlation between Tyr and G6P (r = −0.505),Cit (r = −0.703), Succ (r = −0.483), and Mal (r = −0.299). These correlations provide circumstantial evidence that such amino acids are catabolized to likely generate carbon skeletons and consequently can produce energy via the Tricarboxylic Acid (TCA) cycle.

The principal component analysis (PCA), performed by the Euclidian distance considering ~70% similarity, showed three distinct groups, one formed by the genotype CNPAE183 at concentrations of 0 dS m^{-1} and 10 dS m^{-1}, *i.e.*, both extreme conditions. A second group encompasses the CNPAE183 genotype at concentrations of 2.5 dS m^{-1}, 5 dS m^{-1} and 7.5 dS m^{-1}, together with the JCAL171 genotype at concentrations of 7.5 dS m^{-1} and10 dS m^{-1} and a third group consisting essentially of the CNPAE218 genotype (Supplementary Fig. S5). This figure shows the loading plot that each of the components had on the formation of each group. This loading plot shows that the separation of the genotype CNPAE218 was essentially promoted by A_N, VPD, T_{leaf}, and $\delta^{13}C$, whereas the profile of amino acids and organic acids promoted the separation of genotype CNPAE183 from the other genotypes. These components strongly influenced the separation of the CNPAE218 genotype because of its high loading plot, which is 0.223, 0.129, 0.131 and 0.218 for A_N, VPD, T_{leaf}, and $\delta^{13}C$, respectively. On the other hand, the strong participation of Ribose 5-Phosphate (0.408) and Trp (0.403) contributed to the separation of genotype CNPAE183 (Supplementary Fig. S5 and Supplementary Table S3).

4. Discussion

4.1. Salt stress affected net photosynthesis in J. curcas

The response of A_N to salinity depend on the severity and duration of the stress, and thus photosynthetic impairments have been directly related not only to stomatal and mesophyll limitations but also to biochemical limitations (Flexas et al., 2016). In fact, A_N is one of the primary processes affected by salt stress in *J. curcas* (Silva et al., 2015; Campos et al., 2012; Cerqueira et al., 2019). Our results indicate that photosynthetic impairments in *J. curcas* in response to salt stress are likely mediated by plastic responses occurring at the level of stomata (Fig. 1).

An increased number of small stomata, as observed here likely required to improve gaseous CO_2 diffusion into leaves and to sustain higher rates of A_N as revealed by the negative correlation between g_s and stomatal density (r = −0.542), stomatal area (r = −0.379), and maximum pore area (r = −0.141). This evidence is further confirmed by negative correlation between T and stomatal density (r = −0.227), stomatal area (r = −0.507), and maximum pore area (r = −0.307). Although, these results are in agreement with Franks, Drake and Beerling (Franks et al., 2009), it is, however, in contrast with halophyte

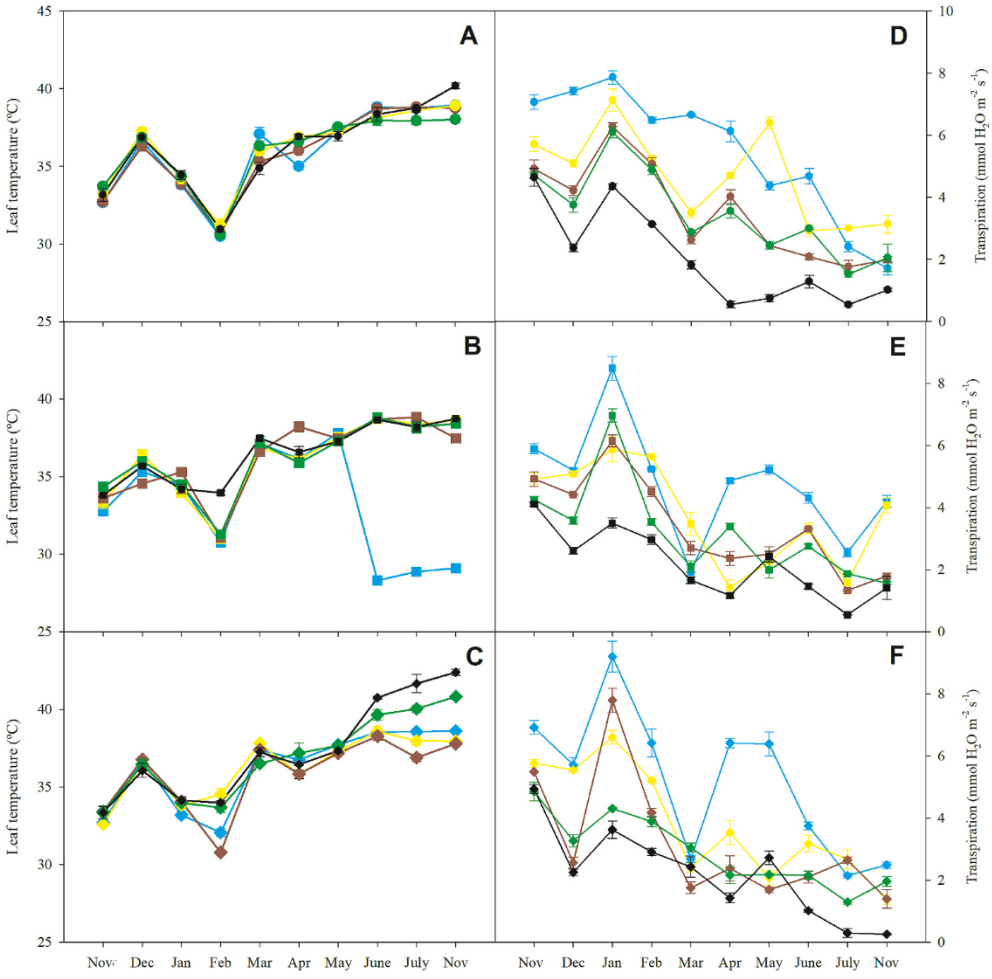

Fig. 4. Salt stress induced changes in leaf temperature and transpiration in *Jatropha curcas* Leaf temperature (A–C) and transpiration (D–F) measured in three genotypes (CNPAE183 – ●, A; JCAL171 – ■, B, and CNPAE218 – ◆ C) of *Jatropha curcas* subjected to five concentration of salt [0 dS m^{-1} (cyan), 2.5 dS m^{-1} (yellow), 5 dS m^{-1} (brown), 7.5 dS m^{-1} (light green), and 10 dS m^{-1} (black)] in water irrigation during the experiment. All data are expressed as means ± SE (n = 5). For statistical analysis, see Supplementary Table S1. (For interpretation of the references to color in this figure legend, the reader is referred to the Web version of this article.)

studies, like as quinoa (Shabala et al., 2013), amaranth (Omami et al., 2006) and other species (Shabala, 2013).

We further observed an increased rate of transpiration in the genotype CNPAE183 suggesting an enhanced leaf cooling capacity under salt stress (Fig. 4). Increased stomatal density with a reduction of its stomatal size (Fig. 1F) was further observed in this genotype, whereas the other genotypes increase its stomatal density with a linear increase in stomatal size. Increased rates of transpiration and leaf cooling regardless of the genotype in *J. curcas* grown under salinity conditions resulted from differences in stomatal size and/or stomatal opening capacity.

Generally, larger stomata close slowly as compared to the smaller stomata (Franks et al., 2009; Drake et al., 2013); thus the relatively large stomata of *J. curcas* leaves (Hsie et al., 2015) might result in excessive leaf desiccation if large stomatal apertures are observed. We observed here that the increase in T_{leaf} is likely due to reduced evapotranspiration cooling in response to salt stress. This physiological response to increasing salt stress can prevent the lethal stress effects caused by salinity especially under sunny conditions. Hence, lower T_{leaf} in tolerant genotypes might be the adaptation mechanism that allow *J. curcas* to maintain enough leaf water that permit greater stomatal opening and ultimately allow constant transpirational cooling as well as CO_2 influx towards the chloroplasts for periods longer, and thus allowing greater A_N.

The lower T_{leaf} observed in the tolerant genotypes may result from mechanisms that maintain a more favorable leaf water status and, therefore, allow greater stomatal opening that sustained not only transpirational cooling, but also the influx of CO_2 towards the chloroplasts for periods longer, allowing greater A_N (Hsie et al., 2015; Franks et al., 2009; Drake et al., 2013).

Reduction in A_N cannot be solely related to the decrease in the acquisition of CO_2 due to stomatal closure since the stomata can remain open at moments of lower VPD (Hsie et al., 2015). The fact that the C_i/C_a ratio linearly increased with the salt concentration ($r = 0.374$) and was more abrupt at higher salt concentrations (Fig. 3) most likely largely overcome limitations to CO_2 diffusion throughout the mesophyll in *J. curcas*. Additionally, the reduction of Rubisco carboxylative activity can be linked to the lower water status of salt-stressed plants that affect the maintenance of the metabolic activities. Reductions in A_N as observed in present study, could be connected to the dysfunctions at the level of biochemical reactions associated with CO_2 fixation due possibly to limitations in RuBP synthesis caused by ATP deficiency, as suggested to occur under severe drought conditions (Lawlor and Tezara, 2009). In good agreement, the reductions in A_N may be associated with the lower availability of NADPH and ATP, since both Φ_{PSII} and ETR decreased as a consequence of salinity ($r = -0.404$ to Φ_{PSII} and $r = -0.392$ to ETR; Supplementary Data File). Net photosynthesis is the preferred pathway for electrons under the optimal conditions, however, A_N is very sensitive and decreases rapidly than ETR under stress condition and thus promote an increase in the ETR/A_N ratio, which indicate that energy compromise takes place and thus it can be linked to the ROS production (Fonseca-Pereira et al., 2019). ETR/A_N ratio reflects the energy transfer to A_N and an increase in this ratio, as noted here in the CNPAE183 genotype, indicates that alternative electron sinks most likely increased due to the stressful conditions caused by NaCl (Silva et al., 2015; Cerqueira et al., 2019).

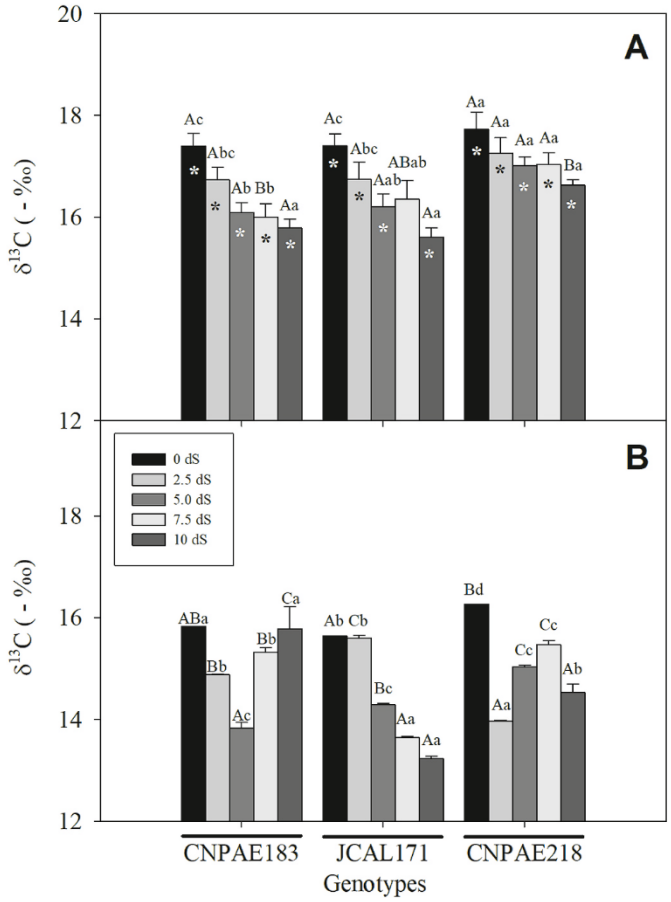

Fig. 5. Salt stress induced changes in Carbon isotope ratio ($\delta^{13}C$) in *Jatropha curcas*. $\delta^{13}C$ was measured in three genotypes (CNPAE183, JCAL171, and CNPAE218) of *Jatropha curcas* subjected to five concentration of NaCl (0 dS m^{-1}, 2.5 dS m^{-1}, 5 dS m^{-1}, 7.5 dS m^{-1} e 10 dS m^{-1}). For each plant, an expanding leaf were collected 6 (A) and 12 (B) months after start of salt irrigation of plants. The measurements were taken at midday. All data are expressed as means ± SE (n = 5). Different lowercase letters denote significance within salt concentration for each genotype, and different capital letters denote significance within genotype for the same salt concentration. Asterisks denote significance within the same treatment in the two sampling periods.

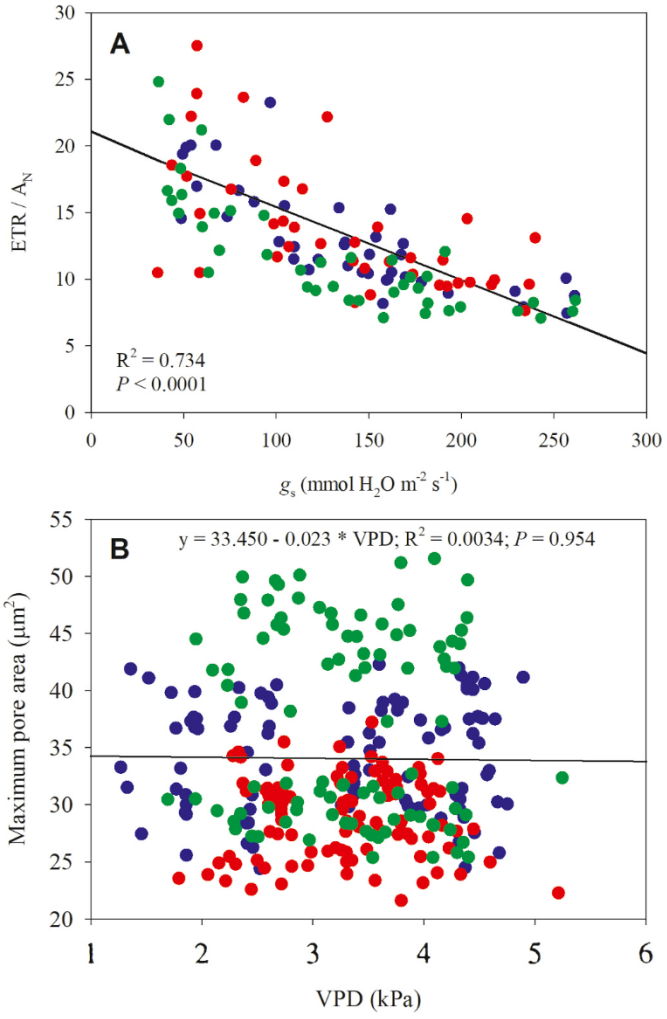

Fig. 6. Relationship between the ratio of electron transport rate (ETR) and net photosynthesis (A_N) *versus* stomatal conductance (g_s) (A) and between the water vapor difference between the plant and the atmosphere (DPV) and ostiole opening (B) measured in three genotypes (CNPAE183, red symbols; JCAL171, blue symbols, and CNPAE218, green symbols) of *Jatropha curcas* subjected to five concentration of NaCl (0 dS m^{-1}, 2.5 dS m^{-1}, 5 dS m^{-1}, 7.5 dS m^{-1} e 10 dS m^{-1}). Data represent averages of five biological replicates per genotype and conditions. Regression coefficient (R^2) and *P* value are shown. (For interpretation of the references to color in this figure legend, the reader is referred to the Web version of this article.)

4.2. Salt stress modulate catabolism in *J. curcas*

Significant efforts have been expended to comprehend mechanisms associated with salinity tolerance responses in various plant species (Muchate et al., 2016; Munns et al., 2020; van Zelm et al., 2020). In response to salt stress, impairments in both physiological and metabolic activities due to osmotic stress, ionic stress, nutritional imbalances, or a combination of these factors are usually observed (Slama et al., 2015). Our main goal here was to enhance our understanding of the importance of physiological and metabolic responses to salt stress in *J. curcas* genotypes. Therefore, we first demonstrated that significant accumulation of both Na^+ and Cl^- in leaf samples in all genotypes occurred following salt stress and this accumulation is lower in the tolerant genotype CNPAE183 (Fig. 7). It is widely known that in plant tissues adequate ratios of K^+/Na^+ (usually above 1.0) in the presence of NaCl are important for both K^+/Na^+ homeostasis and tolerance to salinity (Silva et al., 2015). Moreover, K^+/Na^+ discrimination during xylem loading may increase the levels of compatible solutes (Chen et al., 2007). Accordingly, an ionic imbalance coupled with low tolerance under moderate to severe salt stress were previously described in *J. curcas* (Silva et al., 2015). Notably, in the salt-tolerant genotype CNPAE183 the K^+/Na^+ ratio reached values above 1.2 and in the genotype JCAL171 a higher K^+/Na^+ ratio (up to 2.4) were observed suggesting a strong connection between ion homeostasis and salinity tolerance in those genotypes. K^+/Na^+ ratio below 0.9 in the CNPAE218 genotype provide further support to our motion that this genotype failed to establish a favorable ionic balance under salt stress.

We further observed an interesting metabolic reprogramming in *J. curcas* during salt stress. Briefly, an increase in Ser in both CNPAE183 and JCAL171 genotypes whereas a high reduction in the CNPAE218 genotype, suggest that the in the former genotypes photorespiration may act reducing power generated during the photochemical phase of the photosynthesis. In fact, photosynthesis related reactions, including light reactions, the Calvin-Benson cycle, and photorespiration, were strongly downregulated following salt stress (Batista-Silva et al., 2018). Since photorespiration protects the chloroplast against excessive light energy and possibly acts as a ROS-scavenging mechanism to cope with the excess of energy in impaired photosystems under salt stress, it seems reasonable to assume that higher photorespiration, as depicted by increased levels of Ser, may explain, at least partially, salt tolerance in

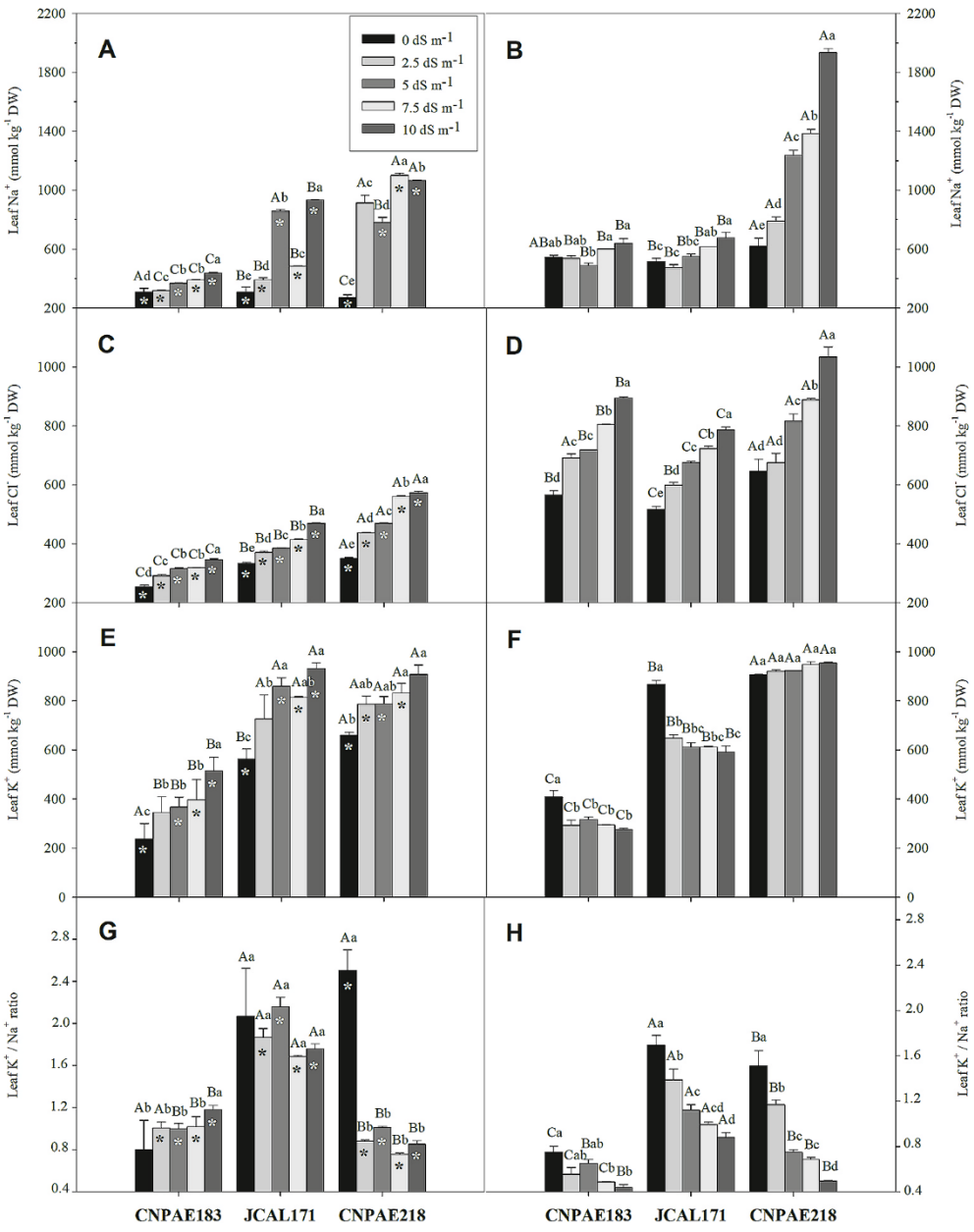

Fig. 7. Salt stress induced changes in nutrients in *Jatropha curcas*. Content of Na^+, Cl^-, K^+ and K^+/Na^+ ratio measured in three genotypes (CNPAE183, JCAL171, and CNPAE218) of *Jatropha curcas* subjected to five concentration of NaCl (0 dS m^{-1}, 2.5 dS m^{-1}, 5 dS m^{-1}, 7.5 dS m^{-1} e 10 dS m^{-1}). All data are expressed as means ± SE (n = 5). Different lowercase letters denote significance within salt concentration for each genotype, and different capital letters denote significance within genotype for the same salt concentration. An asterisk (*) denote significance within 6- and 12-months plants in the same treatment.

J. curcas.

During abiotic stress, low abundance amino acids are not synthesized but rather accumulated due to an increased protein turnover (Hildebrandt, 2018). Interestingly, our results demonstrated a negative correlation ($r = -0.693$) between proteins and amino acids pool. Moreover, polyamines, namely Putrescine (Put), Spermidine (Spd), and Spermine (Spm), are involved not only in plant growth and development, but also in stress responses (Yuan et al., 2019). Polyamine-induced salt tolerance is closely related to the regulation of intracellular ion homeostasis in plants (Yuan et al., 2019). In close agreement, plants from the genotypes CNPAE183 and JCAL171 showed salinity tolerance since when subjected to 5 dS m^{-1} they accumulated up to 4.8- and 4.1-fold more Put than control plants (Fig. 8) and a positive correlation between saline concentration and Put ($r = 0.434$) was further observed.

Not only protein degradation but also the metabolism of branched-chain amino acids (BCAAs) and Lys are strongly induced during salt stress (Huang et al., 2019; Hildebrandt, 2018). High levels of ATP is promoted by oxidation of BCAAs and Lys, which is considered as another auxiliary pathway that can be activated when the main pathway (photosynthesis) is impaired and thus benefits the survival of salt-stressed plants (Hildebrandt et al., 2015). We observed a positive correlation between salt concentration and Lys ($r = 0.546$) and a negative correlation between Lys and Glu ($r = -0.609$), Isoc ($r = -0.418$), G6P ($r = -0.300$), Succ ($r = -0.379$), and Mal ($r = -0.820$). Higher accumulation of BCAAs during transient osmotic stress clearly implies tight regulation of BCAA catabolism as potential energy sources for plants. It has been demonstrated that an upregulation of BCAA catabolism occurs during senescence or under carbon starvation and thereby provides skeleton carbon for plants during stress conditions (Hildebrandt et al., 2015). In agreement with the idea that salt stress is likely culminating also with carbon starvation, it has been recently demonstrated that one gene for Suc synthesis and four genes for starch synthesis were downregulated in JCAL171 *J. curcas* plants, whereas there was no differential expression in the genotype CNPAE183 between control plants and following 3 h of exposure to 150 mM NaCl (Souza et al., 2020).

Proteins degradation is reported in stressed-plants and the complete oxidation of their amino acids could supply energy for the particular

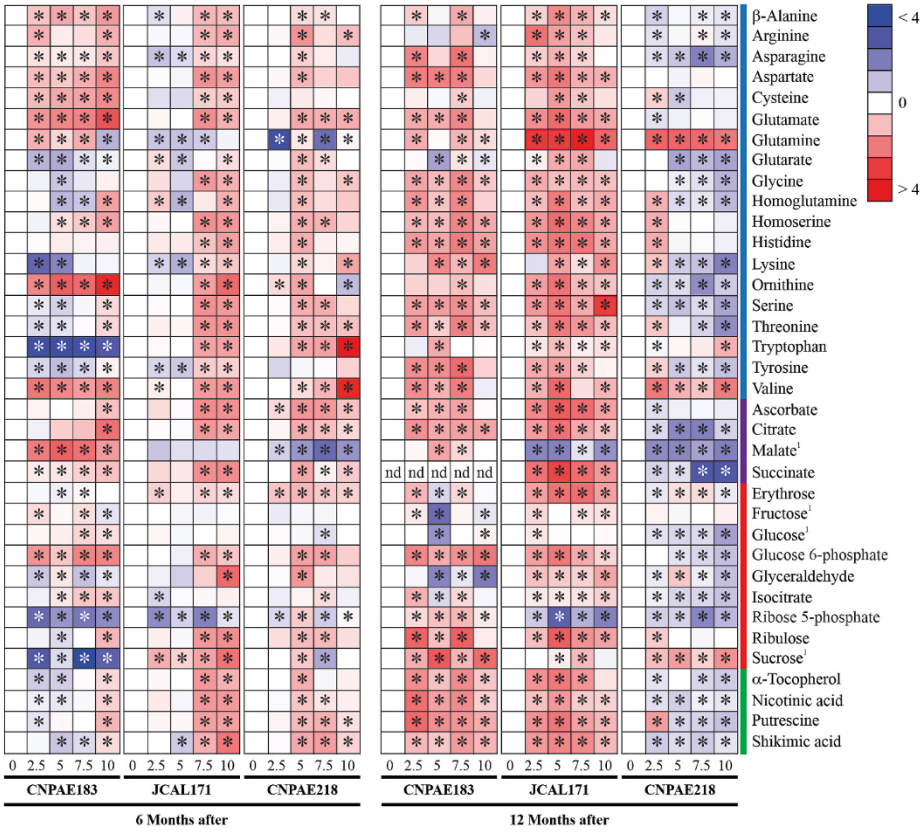

Fig. 8. Heat map representing the salt induced changes in relative metabolite abundance of primary metabolite levels in *Jatropha curcas*. Metabolites content were determined in three genotypes (CNPAE183, JCAL171 and CNPAE218) of *Jatropha curcas* subjected to five concentration of NaCl (0 dS m^{-1}, 2.5 dS m^{-1}, 5.0 dS m^{-1}, 7.5 dS m^{-1} e 10 dS m^{-1}). The data were evaluated 6 and 12 months after saline irrigation. The color code of the heat map is given at the log(2) following the scale. Data are normalized with respect to the mean response calculated for control (0 dS m^{-1} of each genotype in which time). To allow statistical assessment, individual plants from this set were normalized in the same way. Values represented means ± SE (SNK; $P \leq 0.05$) of four biological replicates. An asterisk (*) indicate that the values from other samples to be significantly different for its control ones. nd. not detected. [1] The compound were enzymatically measured and denote absolute value not relative values. For all statistical analysis, see Supplementary Table S2. (For interpretation of the references to color in this figure legend, the reader is referred to the Web version of this article.)

needs of certain organs (Hildebrandt et al., 2015; Araújo et al., 2011). We observed here strong positive correlations between several amino acids and energetic related compounds (*e.g.* G6P, Glyc, Cit, Isoc, and Mal). Thus, we suggest that in response to salt stress, protein degradation occurred increasing amino acid content that not only represent building blocks for several other biosynthesis pathways but also intermediates during signaling processes as well as in the stress responses (Hildebrandt et al., 2015; Araújo et al., 2011; Häusler et al., 2014).

There is a consensus (Lin et al., 2018; Sivakumar et al., 2000) that NaCl can inhibit some enzymes of the Calvin-Benson cycle. A schematic summary model that explain that decrease photosynthesis through inhibition of some enzymes promoted by salt-stress are presented in Graphical abstract. Briefly, salt stress appears to inhibit Rubisco, Fructose 1,6-Bisphosphatase, Sedoheptulose 1,7-Bisphosphatase, Transketolase and finally Ribulose 5-Phosphate Isomerase (Lin et al., 2018; Sivakumar et al., 2000). The last enzyme catalyzes the conversion between Ribose 5-Phosphate and Ribulose 5-Phosphate. Our results revealed that CNPAE183 genotype increased Ribose 5-Phosphate by 3.8-fold when compared with control samples, while the CNPAE218 genotype decreased by 55%. This schematic model further indicated that some amino acids can feed carbon skeletons to TCA, as it strongly occurred in the genotype CNPAE183 and moderately in genotype JCAL171, differing from CNPAE218, which reduced the great majority of free amino acids (Fig. 8).

Several proteome and transcriptome changes were observed due to salt stress and this is caused by changes in metabolic system due to salinity Yang, Ma, Wang, Chen and Li (Yang et al., 2012). The response pattern described by Yang, Ma, Wang, Chen and Li (Yang et al., 2012) is seemingly similar to those presented by Lin, Li, Yuan, Yang, Wang and Chen (Lin et al., 2018) and those presented here. Our results are highly consistent with those described previously (Silva et al., 2015; Cerqueira et al., 2019; Corte-Real et al., 2020), which demonstrated that *J. curcas* is a species that display important photoprotective mechanisms to cope with the harmful effects of salinity. These attributes are mainly due to the great capacity of modulating stomatal characteristics in response VPD (Hsie et al., 2015). The ability to cope with salt stress is not only associated with the activities of protective enzymes and their defensive functions (Pompelli et al., 2010b; Silva et al., 2015; Campos et al., 2012) but also through the ability to thermally dissipate excess of energy (Cerqueira et al., 2019). Remarkably, the characteristics that led to the separation of the tolerant genotype CNPAE218 from the others were associated with its lowest photosynthetic related parameters (*e.g.* A_N, T_{leaf}, and $\delta^{13}C$) as well as the high metabolic reprogramming towards the synthesis of amino acids and organic acids. Taken together, the results described here coupled with previous studies (Campos et al., 2012; Corte-Real et al., 2020; Souza et al., 2020) indicate that salt stress tolerance in *J. curcas* is likely mediated by an effective antioxidative and photoprotective system.

Author contributions

MFP and LE manage project finances. MFP, PPBF, ARMC, LE conceived and designed the experiments. MFP, PPBF, and ARMC performed most of the experiments, with the support of AOM, and WBS. MFP, RCQQF, KRM, AOM, AJO, and WBS analyzed the data and discussed the results. MFP, LE, and WLA wrote the manuscript, which was later approved by all the others.

Declaration of competing interest

The authors declare that they have no known competing financial interests or personal relationships that could have appeared to influence the work reported in this paper.

Acknowledgments

This work was made possible through financial support from the National Council for Scientific and Technological Development (CNPq-

Brazil, Grant 404357/2013–0). We thank the scholarships granted by CNPq-Brazil (Grants 163524/2017–3 to MFP) and Foundation for Science and Technology of Pernambuco (Grants IBPG-1737-2.07/15 to PPBF). Research fellowship granted by CNPq-Brazil to WA is also gratefully acknowledged. We additionally acknowledge Embrapa Agroenergia (Brasília, DF, Brazil) for donating the *J. curcas* seeds and Embrapa Semiárido, Petrolina, PE, Brazil for providing all infrastructure for the assembly of this study. In addition, the authors extend special thanks to Nucleus of Microscopy and Microanalyses, at the Universidade Federal de Viçosa for technical assistance and Dr Karina Lidianne Alcântara Saraiva (Technology Platforms Nucleus, Aggeu Magalhães Institute) and MsC. Ana Carla da Silva (Cell Biology of Pathogens Laboratory, Aggeu Magalhães Institute) for their help with scanning electron microscopy procedures.

Appendix A. Supplementary data

Supplementary data to this article can be found online at https://doi.org/10.1016/j.plaphy.2021.09.039.

References

Aguiar Neto, P., Grangeiro, L.C., Mendes, L.M.S., Costa, N.D., Marrocos, S.T.P., Sousa, V. F.L., 2014. Crescimento e acúmulo de macronutrientes na cultura da cebola em Baraúna (RN) e Petrolina (PE). Rev. Bras. Eng. Agrícola Ambient. 18, 370–380.

Alburquerque, N., García-Almodóvar, R.C., Valverde, J.M., Burgos, L., Martínez-Romero, D., 2017. Characterization of *Jatropha curcas* accessions based in plant growth traits and oil quality. Ind. Crop. Prod. 109, 693–698.

Araújo, W.L., Tohge, T., Ishizaki, K., Leaver, C.J., Fernie, A.R., 2011. Protein degradation - an alternative respiratory substrate for stressed plants. Trends Plant Sci. 16, 489–498.

Batista-Silva, W., Heinemann, B., Rugen, N., Nunes-Nesi, A., Araújo, W.L., Hildebrandt, T.M., 2018. The role of amino acid metabolism during abiotic stress release. Plant Cell Environ. 42, 1630–1644.

Bradford, M., 1976. A rapid and quantitative method for quantitation of microgram quantities of protein utilizing the principle of protein-dye binding. Anual Biochem 72, 284-252.

Cabral, G.A.L., Binneck, E., Souza, M.C.P., Silva, M.D., Ferreira Neto, J.R.C., Pompelli, M. F., Endres, L., Kido, E.A., 2020. First expressed TFome of physic nut (*Jatropha curcas* L.) after salt stimulus. Plant Mol. Biol. Rep. 38, 189–208.

Campos, M.L.O., Hsie, B.S., Granja, J.A.A., Correia, R.M., Silva, S.R.S., Almeida-Cortez, J. S., Pompelli, M.F., 2012. Photosynthesis and antioxidant activity mechanisms in *Jatropha curcas* L. under salt stress. Braz. J. Plant Physiol. 24, 55–67.

Cerqueira, J.V.A., Silveira, J.A.G., Carvalho, F.E.L., Cunha, J.R., Lima Neto, M.C., 2019. The regulation of P700 is an important photoprotective mechanism to NaCl-salinity in *Jatropha curcas*. Physiol. Plantarum 167, 404–417.

Chen, Z., Zhou, M., Newman, I.A., Mendham, N.J., Zhang, G., Shabala, S., 2007. Potassium and sodium relations in salinised barley tissues as a basis of differential salt tolerance. Funct. Plant Biol. 34, 150–162.

Cheng, Y., Chen, G., Hao, D., Lu, H., Shi, M., Mao, Y., Huang, X., Zhang, Z., Xue, L., 2014. Salt-induced root protein profile changes in seedlings of maize inbred lines with differing salt tolerances. Chil. J. Agric. Res. 74, 468–476.

Corte-Real, N., Endres, L., Santos, K.P.O., Figueirêdo, R.C.B., Arruda, E.C.P., Ulisses, C., Pompelli, M.F., 2016. Morphoanatomy and ontogeny of the fruit and seeds of *Jatropha curcas* L.: a promising biofuel plant. In: Segura-Campos, M.R., Betancur-Ancova, D. (Eds.), The Promising Future of *Jatropha Curcas*: Proprieties and Potential Applications. Nova Science Publishers, Inc., Hauppauge, NY, pp. 141–158.

Corte-Real, N., Miranda, P.V.V.C., Endres, L., Souza, E.R., Pompelli, M.F., 2019. Tolerance to salinity in *Jatropha curcas* are genotype-dependent. Braz J Develop 5, 22169–22199.

Corte-Real, N., Oliveira, M.S., Jarma-Orozco, A., Fernandes, D., dos Santos, M.A., Endres, L., Calsa Jr., T., Pompelli, M.F., 2020. Comparative analysis of salt-induced changes in the leaves proteome of two contrasting *Jatropha curcas* genotypes. Braz J Develop 6, 39845–39872.

Drake, P.L., Froend, R.H., Franks, P.J., 2013. Smaller, faster stomata: scaling of stomatal size, rate of response, and stomatal conductance. J. Exp. Bot. 64, 495–505.

Ehleringer, J.R., White, J.W., Johnson, D.A., Brick, M., 1990. Carbon isotope discrimination, photosynthetic gas exchange, and transpiration efficiency in beans and range grasses. Acta Oecol. 11, 611–625.

Fernie, A.R., Roscher, A., Ratcliffe, R.G., Kruger, N.J., 2001. Fructose 2,6-bisphosphate activates pyrophosphate: fructose-6-phosphate 1-phosphotransferase and increases triose phosphate to hexose phosphate cycling heterotrophic cells. Planta 212, 250–263.

Flexas, J., Díaz-Espejo, A., Conesa, M.A., Coopman, R.E., Douthe, C., Gago, J., Gallé, A., Galmés, J., Medrano, H., Ribas-Carbo, M., Tomàs, M., Niinemets, Ü., 2016. Mesophyll Conductance to CO_2 and Rubisco as Targets for Improving Intrinsic Water Use Efficiency in C3 Plants, Plant, vol. 39. Cell & Environment.

Fonseca-Pereira, P., Daloso, D.M., Gago, J., Nunes-Nesi, A., Araújo, W.L., 2019. On the role of the plant mitochondrial thioredoxin system during abiotic stress. Plant Signal. Behav. 6, 1592536.

Franks, P.J., Drake, P.L., Beerling, D.J., 2009. Plasticity in maximum stomatal conductance constrained by negative correlation between stomatal size and density: an analysis using *Eucalyptus globulus*. Plant Cell Environ. 32, 1737–1748.

Häusler, R.E., Ludewig, F., Krueger, S., 2014. Amino acids - a life between metabolism and signaling. Plant Sci. 229, 225–237. https://doi.org/10.1016/j.plantsci.2014.09.011. Plant Sci, 229 (2014) 225-237.

Hildebrandt, T.M., 2018. Synthesis versus degradation: directions of amino acid metabolism during *Arabidopsis* abiotic stress response. Plant Mol. Biol. 98, 121–135.

Hildebrandt, T.M., Nunes-Nesi, A., Araújo, W.L., Braus, H.-P., 2015. Amino acid catabolism in plants. Mol. Plant 8, 1563–1579.

Hsie, B.S., Mendes, K.R., Antunes, W.C., Endres, L., Campos, M.L.O., Souza, F.C., Santos, N.D., Singh, B., Arruda, E.C.P., Pompelli, M.F., 2015. *Jatropha curcas* L. (Euphorbiaceae) modulates stomatal traits in response to leaf-to-air vapor pressure deficit. Biomass Bioenergy 81, 273–281.

Huang, L., Li, Z., Liu, Q., Pu, G., Zhang, Y., Li, J., 2019. Research on the adaptive mechanism of photosynthetic apparatus under salt stress: new directions to increase crop yield in saline soils. Ann. Appl. Biol. 175, 1–17.

Karnovsky, M.J., 1965. A formaldehyde-glutaraldehyde fixative of high osmolality for use in electron microscopy. J. Cell Biol. 27, 137–138.

Koca, H., Bor, M., Özdemir, F., Türkan, I., 2007. The effect of salt stress on lipid peroxidation, antioxidative enzymes and proline content of sesame cultivars. Environ. Exp. Bot. 60, 344–351.

Koppen, W., 1948. Climatologia: con un estudio de los climas de la tierra. Fondo de Cultura Economica, Mexico.

Laviola, B.G., Alves, A.A., Rosado, T.B., Bhering, L.L., Formighieri, E.F., Peixoto, L.A., 2018. Establishment of new strategies to quantify and increase the variability in the Brazilian *Jatropha* genotypes. Ind. Crop. Prod. 117, 216–223.

Lawlor, D.W., Tezara, W., 2009. Causes of decreased photosynthetic rate and metabolic capacity in water-deficient leaf cells: a critical evaluation of mechanisms and integration of processes. Ann. Bot. 103, 561–579.

Lin, J., Li, J.P., Yuan, F., Yang, Z., Wang, B.S., Chen, M., 2018. Transcriptome profiling of genes involved in photosynthesis in *Elaeagnus angustifolia* L. under salt stress. Photosynthetica 56, 998–1009.

Lisec, J., Schauer, N., Kopka, J., Willmitzer, L., Fernie, A.R., 2006. Gas chromatography mass spectrometry-based metabolite profiling in plants. Nat. Protoc. 1, 387–396.

Lozano-Isla, F., Campos, M.L.O., Endres, L., Bezzera-Neto, E., Pompelli, M.F., 2018. Effects of seed storage time and salt stress on the germination of *Jatropha curcas* L. Ind. Crop. Prod. 118, 214–224.

Muchate, M.S., Nikalje, G.C., Rajurkar, N.S., Suprasanna, P., Nikam, T.D., 2016. Plant salt stress: adaptive responses, tolerance mechanism and bioengineering for salt tolerance. Bot. Rev. 82, 371–406.

Munns, R., Passioura, J., Colmer, T., Byrt, C., 2020. Osmotic adjustment and energy limitations to plant growth in saline soil. New Phytol. 225, 1091–1096.

Niu, L., Tao, Y.-B., Chen, M.-S., Fu, Q., Dong, Y., He, H., Xu, Z.-F., 2016. Identification and characterization of tetraploid and octoploid *Jatropha curcas* induced by colchicine. Caryologia 69, 58–66.

Nunes-Nesi, A., Carrari, F., Gibon, Y., Sulpice, R., Lytovchenko, A., Fisahn, J., Graham, J., Ratcliffe, R.G., Sweetlove, L.J., Fernie, A.R., 2007. Deficiency of mitochondrial fumarase activity in tomato plants impairs photosynthesis via an effect on stomatal function. Plant J. 50, 1093–1106.

Omami, E.N., Hammes, P.S., Robbertse, P.J., 2006. Differences in salinity tolerance for growth and water-use efficiency in some amaranth (*Amaranthus* spp.) genotypes. N. Z. J. Crop Hortic. Sci. 34, 11–22.

Pandey, V.C., Singh, K., Singh, J.S., Kumar, A., Singh, B., Singh, R.P., 2012. *Jatropha curcas*: a potential biofuel plant for sustainable environmental development. Renew. Sustain. Energy Rev. 16, 2870–2883.

Pompelli, M.F., Ferreira, D.T.R.G., Cavalcante, P.P.G.S., Salvador, T.L., Hsie, B.S., Endres, L., 2010a. Environmental influence on the physico-chemical and physiological properties of *Jatropha curcas* L. seeds. Aust. J. Bot. 58, 421–427.

Pompelli, M.F., Barata-Luís, R.M., Vitorino, H.S., Gonçalves, E.R., Rolim, E.V., Santos, M. G., Almeida-Cortez, J.S., Endres, L., 2010b. Photosynthesis, photoprotection and antioxidant activity of purging nut under drought deficit and recovery. Biomass Bioenergy 34, 1207–1215.

Pompelli, M.F., Martins, S.C., Celin, E.F., Ventrella, M.C., DaMatta, F.M., 2010c. What is the influence of ordinary epidermal cells and stomata on the leaf plasticity of coffee plants grown under full-sun and shady conditions? Braz. J. Biol. 70, 1083–1088.

Pompelli, M.F., Martins, S.C.V., Antunes, W.C., Chaves, A.R.M., DaMatta, F.M., 2010d. Photosynthesis and photoprotection in coffee leaves is affected by nitrogen and light availabilities in winter conditions. J. Plant Physiol. 167, 1052–1060.

Proclima, 2020. Programa de Monitoramento Climático em Tempo Real da Região Nordeste. Instituto Nacional de Pesquisas Espaciais, São José dos Campos.

Rengasamy, P., 2010. Soil processes affecting crop production in salt-affected soils. Funct. Plant Biol. 37, 613–620.

Reubens, B., Achten, W.M.J., Maes, W.H., Danjon, F., Aerts, R., Poesen, J., Muys, B., 2011. More than biofuel? *Jatropha curcas* root system symmetry and potential for soil erosion control. J. Arid Environ. 75, 201–205.

Salisbury, E.J., 1928. On the causes and ecological significance of stomatal frequency, with special reference to the woodland flora. Philos T R Soc B 216, 1–65.

Schmook, B., Seralta-Peraza, L., 1997. *J. curcas*: distribution and uses in the Yucatan Peninsula of Mexico. In: Gübitz, G.M., Mittelbach, M., Trabi, M. (Eds.), Biofuels and Industrial Products from *Jatropha Curcas*. Dbv-Verlag für die Technische Universität Graz, Berlin, pp. 53–57.

Shabala, S., 2013. Learning from halophytes: physiological basis and strategies to improve abiotic stress tolerance in crops. Ann. Bot. 112, 1209–1221.
Shabala, S., Hariadi, Y., Jacobsen, S.-E., 2013. Genotypic difference in salinity tolerance in quinoa (*Chenopodium quinoa*) is determined by differential control of xylem Na^+ loading and stomatal density. J. Plant Physiol. 170, 906–914.
Silitonga, A.S., Hassan, M.H., Ong, H.C., Kusumo, F., 2017. Analysis of the performance, emission and combustion characteristics of a turbocharged diesel engine fuelled with *Jatropha curcas* biodiesel-diesel blends using kernel-based extreme learning machine. Environ. Sci. Pollut. Res. 24.
Silva, F.C., 2009. Manual de análises químicas de solos, plantas e fertilizantes, 2. Embrapa Informação Tecnológica, Brasília.
Silva, E.N., Silveira, J.A.G., Rodrigues, C.R.F., Viégas, R.A., 2015. Physiological adjustment to salt stress in *Jatropha curcas* is associated with accumulation of salt ions, transport and selectivity of K^+, osmotic adjustment and K^+/Na^+ homeostasis. Plant Biol. 17, 1023–1029.
Silva, F.M.O., Lichtenstein, G., Alseekh, S., Rosado-Souza, L., Conte, M., Suguiyama, V.F., Lira, B.S., Fanourakis, D., Usadel, B., Bhering, L.L., DaMatta, F.M., Sulpice, R., Araújo, W.L., Rossi, M., Setta, N., Fernie, A.R., Carrari, F., Nunes-Nesi, A., 2017. The genetic architecture of photosynthesis and plant growth-related traits in tomato. Plant Cell Environ. 41, 327–341.
Silva-Santos, L., Corte-Real, N., Dias-Pereira, J., Figueiredo, R.C.B.Q., Endres, L., Pompelli, M.F., 2019. Salinity shock in *Jatropha curcas* leaves is more pronounced during recovery than during stress time. Braz J Develop 5, 11359–11369.
Sivakumar, P., Sharmila, P., Pardha-Saradhi, P., 2000. Proline alleviates salt-stress-induced enhancement in Ribulose-1,5-bisphosphate oxygenase activity. Biochem. Biophys. Res. Commun. 279, 512–515.
Slama, I., Abdelly, C., Bouchereau, A., Flowers, T., Savouré, A., 2015. Diversity, distribution and roles of osmoprotective compounds accumulated in halophytes under abiotic stress. Ann. Bot. 115, 433–477.
Souza, M.C.P., Silva, M.D., Binneck, E., Cabral, G.A.L., Iseppon, A.M.B., Pompelli, M.F., Endres, L., Kido, E.A., 2020. RNA-Seq transcriptome analysis of *Jatropha curcas* L. accessions after salt stimulus and unigene-derived microsatellite mining. Ind. Crop. Prod. 147, 112168.
Tang, Y., Bao, X., Wang, S., Liu, Y., Tan, J., Yang, M., Zhang, M., Yu, X., 2019. A physic nut stress-responsive HD-Zip transcription factor, JcHDZ07, confers enhanced sensitivity to salinity stress in transgenic *Arabidopsis*. Front. Plant Sci. 10, 942.
van Zelm, E., Zhang, Y., Testerink, C., 2020. Salt tolerance mechanisms of plants. Annu. Rev. Plant Biol. 71, 403–433.
Wellburn, A.R., 1994. The spectral determination of chlorophyll *a* and *b*, as well as total carotenoids, using various solvents with spectrophotometers of different resolution. J. Plant Physiol. 144, 307–313.
Yang, L., Ma, C., Wang, L., Chen, S., Li, H., 2012. Salt stress induced proteome and transcriptome changes in sugar beet monosomic addition line M14. J. Plant Physiol. 169, 839–850.
Yemm, E.W., Cocking, E.C., Ricketts, R.E., 1955. The determination of amino acids with ninhydrin. Analyst 80, 209–214.
Yuan, Y., Zhong, M., Du, N., Shu, S., Sun, J., Guo, S., 2019. Putrescine enhances salt tolerance of cucumber seedlings by regulating ion homeostasis. Environ. Exp. Bot. 165, 70–82.